Gold-plated processes at photon colliders [1]

E. Boos,[j] A. De Roeck,[b] I.F. Ginzburg,[ℓ] K. Hagiwara,[g]
R.D. Heuer,[e] G. Jikia,[d,2] J. Kwiecinski,[h] D.J. Miller,[i]
T. Takahashi,[f] V.I. Telnov,[c,k] T. Rizzo,[m] I. Watanabe,[a]
P.M. Zerwas[c]

[a] *Akita Keizaihoka University, Akita 010-8515, Japan*

[b] *CERN, CH-1211 Geneva 23, Switzerland*

[c] *DESY, Deutsches Elektronen-Synchrotron, D-22603 Hamburg, Germany*

[d] *Universität Freiburg, Hermann–Herder–Str. 3, D-79104 Freiburg, Germany*

[e] *Universität Hamburg/DESY, II Institut für Experimental Physik, Notkestrasse 85, D-22607 Hamburg, Germany*

[f] *Hiroshima University, 1-3-1 Kagamiyama, Higashi-Hiroshima, 739, Japan*

[g] *Theory Group, KEK, Tsukuba, Ibaraki 305-0801, Japan*

[h] *H. Niewodniczański Institute of Nuclear Physics, Kraków, Poland*

[i] *University College London, London WC1E 6BT, UK*

[j] *Institute of Nuclear Physics, Moscow State University*

[k] *Institute of Nuclear Physics, 630090, Novosibirsk, Russia*

[ℓ] *Sobolev Institute of Mathematics SB RAS, 630090, Novosibirsk, Russia*

[m] *Stanford Linear Accelerator Center, Stanford CA 94309, USA*

Abstract

We review the most important topics and objectives of the physics program of the $\gamma\gamma$, γe collider (photon collider) option for an e^+e^- linear collider.

Key words: Higgs particle; supersymmetry, photon photon; photon electron; W; new particle; pair production; laser; backscatter; linear collider

[1] Talk at the Inter. Workshop on High Energy Photon Colliders, Hamburg, June 14–17, 2000

[2] Corresponding author: jikia@pheno.physik.uni-freiburg.de

1 Introduction

1.1 Photon Colliders

A unique feature of an e^+e^- Linear Colliders (LC) with a center of mass (c.m.s.) energy from a few hundred GeV to several TeV [1–4] is the possibility to transform it to a $\gamma\gamma$, γe collider (Photon Collider) via the process of Compton backscattering of laser light off the high energy electrons (positrons are not needed for photon colliders) [5–7]. Additional material can be found in the review papers [8–23], in the Conceptual(Zero) Design Reports [1–3] and in the proceedings of the workshop on photon colliders held at Berkeley [24] in 1995 and in these proceedings [25].

The maximum energy of the scattered photons is [5,6]

$$\omega_m = \frac{x}{x+1}E_0; \quad x \approx \frac{4E_0\omega_0}{m^2c^4} \simeq 15.3\left[\frac{E_0}{\mathrm{TeV}}\right]\left[\frac{\omega_0}{eV}\right], \tag{1}$$

where E_0 is the electron beam energy and ω_0 the energy of the laser photon. For example, for $E_0 = 250$ GeV, $\omega_0 = 1.17$ eV, i.e. $\lambda = 1.06$ μm (Nd:glass laser), we obtain $x = 4.5$ and $\omega_m = 0.82E_0$.

The high energy photon spectrum becomes more peaked for increasing values of x. It turns out that the value $x \approx 4.8$ is the optimum choice for photon colliders, because for $x > 4.8$ the produced high energy photons create QED e^+e^- pairs in collision with the laser photons, and the $\gamma\gamma$ luminosity [6,8,13] will be reduced. Hence, the maximum c.m.s. energy in $\gamma\gamma$ collisions is about 80% (and 90% in γe collisions) of that in e^+e^- collisions. If smaller photon energies are needed, the same laser can be used when the electron beam energy is decreased. In this case the value of the parameter x also decreases and the photon spectrum becomes less peaked. Alternatively, a laser with a shorter wave length may be used to retain the same sharp spectrum ($x \sim 4.8$) at lower energy.

A typical luminosity distribution in $\gamma\gamma$ collisions is characterized by a high energy peak and a low energy part, Ref.[23]. The peak has a width at half maximum of about 15%. The photons in the peak can have a high degree of circular polarization. This peak region is most useful for experimentation. When comparing event rates in $\gamma\gamma$ and e^+e^- collisions we will use the value of the $\gamma\gamma$ luminosity in the peak region $z > 0.8z_m$ where $z = W_{\gamma\gamma}/2E_0$ ($W_{\gamma\gamma}$ being the $\gamma\gamma$ invariant mass) and $z_m = \omega_m/E_0$. The $\gamma\gamma$ luminosity in this region is proportional to the geometric luminosity L_{geom} of the electron beams:

$L_{\gamma\gamma}(z > 0.8z_m) \sim 0.1 L_{ee,geom}$.[3] The geometric luminosity of electron beams in a $\gamma\gamma$ collision region can be made larger than the e^+e^- luminosity because beamstrahlung and beam repulsion are absent for photon beams.

The luminosity of γe collisions is not proportional to the geometric electron-electron luminosity (see the figures in Ref. [23]) even in the high energy part of the luminosity spectrum. This is due to the repulsion of electron beams and beamstrahlung.

The luminosities expected at the TESLA photon collider [23], are presented in Table 1.

Table 1
Parameters of a $\gamma\gamma$ collider based on the TESLA design. The left column refers to $2E_0 = 500$ GeV, the next two columns are useful for Higgs studies with $M_h = 130$ GeV, for at two different values of x.

	$2E_0 = 500$	$2E_0 = 200$	$2E_0 = 158$ GeV
	$x = 4.6$	$x = 1.8$	$x = 4.6$
$L_{ee,geom}, [10^{34}\ \mathrm{cm^{-2}s^{-1}}]$	12.	4.8	3.8
$L_{\gamma\gamma}(z > 0.8z_{m,\gamma\gamma}), [10^{34}\ \mathrm{cm^{-2}s^{-1}}]$	1.15	0.35	0.36
$L_{e\gamma}(z > 0.8z_{m,\gamma e}), [10^{34}\ \mathrm{cm^{-2}s^{-1}}]$	0.97	0.31	0.27

For comparison, the "nominal" e^+e^- luminosity at TESLA at $2E_0 = 500$ GeV is $L_{e^+e^-}(500) = 3\times10^{34}\ \mathrm{cm^{-2}s^{-1}}$ [26]. For the design parameters of the electron beams and the same energy,

$$L_{\gamma\gamma}(z > 0.8z_m) \sim \frac{1}{3} L_{e^+e^-}. \tag{2}$$

For beams with even smaller emittances even higher $\gamma\gamma$ luminosities can be reached, in contrast to the e^+e^- luminosity which is restricted by beam collision effects.

The energy spectrum of high energy photons becomes most strongly peaked if the initial electrons are longitudinally polarized and the laser photons are circularly polarized. This gives almost a factor of 3–4 increase of the luminosity in the high energy peak. The average degree of circular polarization of photons within the high-energy peak amounts to $90-95\%$. The sign of the polarization can easily be changed by changing the signs of both electron and laser photon initial polarizations.

Linear polarization of high energy photons can be obtained by using linearly polarized laser light [7]. The degree of linear polarization at maximum energy

[3] for a thickness of the laser target being equal to one collision length

depends on x: $l_\gamma = 2(1+x)/(1+(1+x)^2)$, giving 0.334, 0.6, 0.8 for $x = 4.8, 2, 1$ respectively. Polarization asymmetries are proportional to l_γ^2, therefore low x values are more preferable for this goal. For $x = 2$ the maximum energy is only 23% lower than for $x = 4.8$, but the signal is 3.2 times larger. So, for energies reduced by 20% compared to $x = 4.8$, significantly larger linear polarization can be achieved.

1.2 Physics Objectives

Recent experiments at the SLC, LEP, the Tevatron and HERA have confirmed to high precision the Standard Model ($\mathcal{SM}$) of the electroweak interactions. In particular, fermion interactions with electroweak gauge bosons of the $\mathcal{SM}$ were verified to per-mille precision.

The central goals of studies at the next generation of e^+e^- colliders are the proper understanding of electroweak symmetry breaking, associated with the problem of mass, and the discovery of new physics beyond the Standard Model [27–29]. Three scenarios are possible for future experiments:

- New particles or interactions will be directly discovered at the TEVATRON and LHC. A linear collider in the e^+e^- and $\gamma\gamma$, γe modes will then play a crucial role in the detailed and thorough study of these new phenomena and in the reconstruction of the underlying fundamental theories.
- LHC and LC will discover and study in detail the Higgs boson but no spectacular signatures of new physics or new particles will be observed. In this case the precision studies of potential deviations of the properties of the Higgs boson, electroweak gauge bosons and the top quark from their Standard Model predictions can provide clues to the physics beyond the $\mathcal{SM}$.
- Electroweak symmetry breaking (EWSB) is a dynamical phenomenon. The interactions of W bosons and t quarks must then be studied at high energies to explore new strong interactions at the TeV scale.

Electroweak symmetry breaking in the $\mathcal{SM}$ is based on the Higgs mechanism, which introduces one elementary Higgs boson. The model agrees with the present data, and the recent global analysis of precision electroweak data in the framework of the $\mathcal{SM}$ [30] suggests a Higgs boson lighter than 200 GeV. A Higgs boson in this mass range is expected to be discovered at the TEVATRON or the LHC. However, it will be the LC in all its modes that tests whether this particle is indeed the $\mathcal{SM}$ Higgs boson or whether it is eventually one of the Higgs states in extended models like the two–Higgs doublet model ($2\mathcal{HDM}$), or the minimal supersymmetric generalization of the $\mathcal{SM}$, $\mathcal{MSSM}$. At least five Higgs bosons are predicted in supersymmetric models, h^0, H^0, A^0, H^+, H^-.

Unique opportunities are offered by the photon collider to search for the heavy Higgs bosons in areas of SUSY parameter space not accessible elsewhere.

In principle, EWSB could also be generated by a strong-coupling theory. In such models, the signals of the EWSB mechanism are most clearly manifest in the properties of the heaviest $\mathcal{SM}$ particles, the W and Z bosons and the t-quark. In that case, measurement of the anomalous electroweak gauge boson and top quark coupling at the LC will be among the most central issues of the physics program.

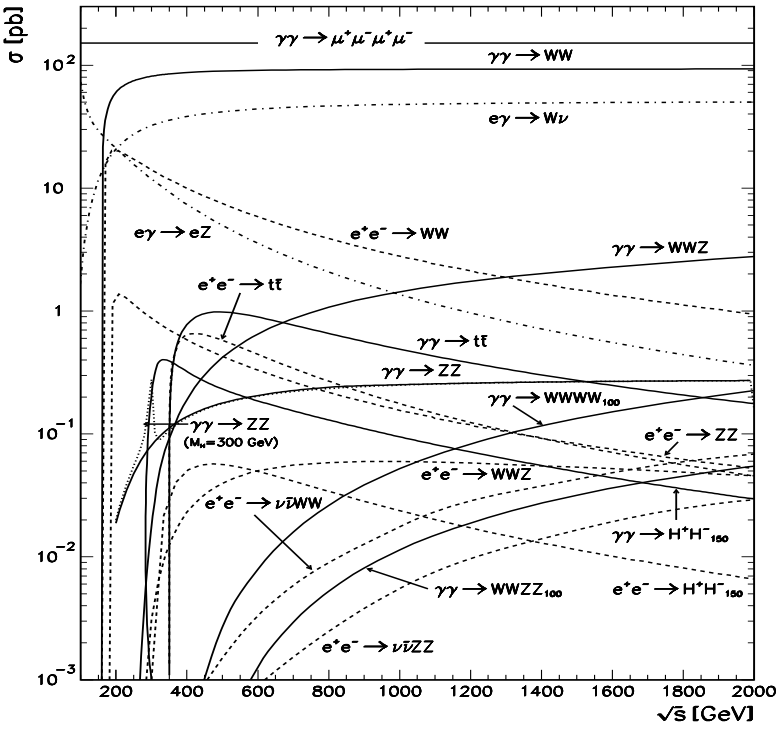

Fig. 1. Typical cross sections in $\gamma\gamma$, γe and e^+e^- collisions. The polarization is assumed to be zero. Solid, dash-dotted and dashed curves correspond to $\gamma\gamma$, γe and e^+e^- modes respectively. Unless indicated otherwise the neutral Higgs mass was taken to be 100 GeV. For charged Higgs pair production, $M_{H^\pm} = 150$ GeV was assumed.

Photon colliders have distinct advantages in searches for and measurements of new physics objects. In general, phenomena in e^+e^- and $\gamma\gamma$, γe collisions are quite similar because the same particles can be produced. However, the reactions are different and often give complementary information. Some phenomena can be studied better at photon colliders due to higher statistical accuracy (based on much larger cross-sections) or due to higher accessible masses (single resonances in $\gamma\gamma$ and γe or a pair of light and heavy particles in γe). A comparison of cross-sections for some processes in e^+e^- and $\gamma\gamma$, γe

collisions are presented in Fig.1 [17].

The cross sections for pairs of scalars, fermions or vectors particles are all significantly larger (about one order of magnitude) in $\gamma\gamma$ collisions than in e^+e^- collisions, as demonstrated in Fig.2 [31,8,11,13].

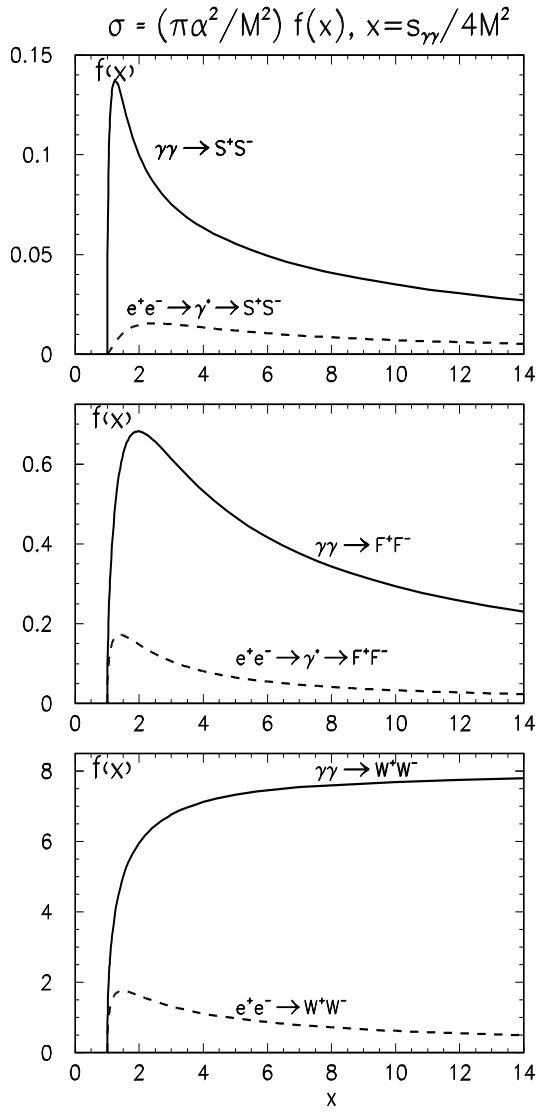

Fig. 2. Comparison between cross sections for charged pair production in unpolarized e^+e^- and $\gamma\gamma$ collisions. S (scalars), F (fermions), W (W bosons); $\sqrt{s}$ is the invariant mass (c.m.s. energy of colliding beams). The contribution of the Z boson to the production of S and F in e^+e^- collisions was not taken into account, it is less than 10%.

For example, the maximum cross section for H^+H^- production with unpolarized photons is about 7 times larger in $\gamma\gamma$ collisions than in e^+e^- collisions (see Fig.1). With polarized photons and not far from threshold, it is even larger by a factor of 20, Fig. 3 [19]. As a result, for the luminosity given in the Table 1

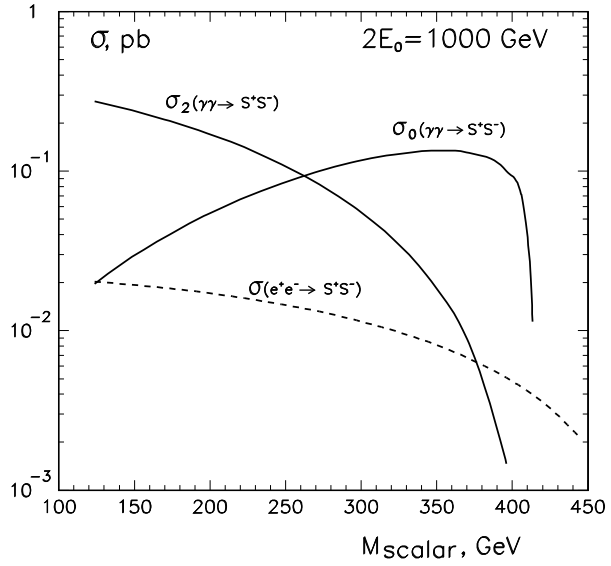

Fig. 3. The pair production cross section for charged scalars in e^+e^- and $\gamma\gamma$ collisions at $2E_0 = 1$ TeV collider energy (in $\gamma\gamma$ collision $W_{max} \approx 0.82$ GeV ($x = 4.6$)); σ_0 and σ_2 correspond to the total $\gamma\gamma$ helicity 0 and 2, respectively.

the event rate is 7 times higher.

The two-photon production of pairs of charged particles is a pure QED process, while the cross section of pair production in e^+e^- collision depends also on the weak isospin of the produced particles via Z exchange, and (sometimes) t–channel exchanges contribute. Therefore, measurements of pair production both in e^+e^- and $\gamma\gamma$ collisions can be exploited to disentangle various couplings of the charged Higgs particles.

Another example is the direct resonant production of the Higgs boson in $\gamma\gamma$ collisions. It is evident from Fig. 4 [18], that the cross section at the photon collider is several times larger than the Higgs production cross section in e^+e^- collisions. Although the $\gamma\gamma$ luminosity is smaller than the e^+e^- luminosity, the production rate of the $\mathcal{SM}$ Higgs boson with mass between 100 and 200 GeV in $\gamma\gamma$ collisions is nevertheless 1–5 times larger than the rate in e^+e^- collisions at $2E_0 = 500$ GeV.

Photon colliders in the γe mode can produce particles which are kinematically not accessible at the same collider in the e^+e^- mode. For example, in γe collisions a heavy charged particle in association with a light neutral particle can be produced, such as a supersymmetric slepton plus a neutralino or a new W' boson and neutrino, and the discovery limits can be extended.

Based on these arguments alone, and without relying on the dynamics *a priori,*

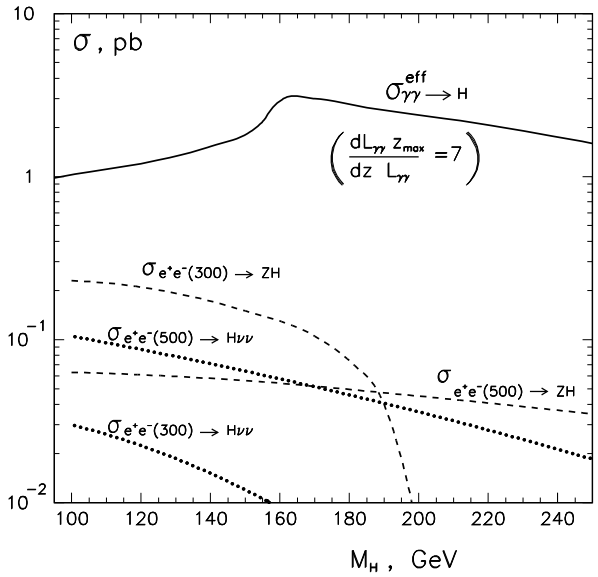

Fig. 4. Total cross sections of the Higgs boson production in $\gamma\gamma$ and e^+e^- collisions. To obtain the Higgs boson production rate at the photon collider, the cross section should be multiplied by the luminosity in the high energy peak $L_{\gamma\gamma}(z > 0.65)$ given in Table 1.

e^+e^- and $\gamma\gamma/\gamma e$ modes are expected to be nicely complimentary for new physics searches. Even though the analyses of new physics scenarios are not yet as advanced in $\gamma\gamma$ and $e\gamma$ collisions as they are for e^+e^- collisions, advantages are obvious for some scenarios.

We present a short summary of the most important objectives and topics of the physics program at the photon collider mode of an LC. We discuss studies of Higgs physics (Section 2), supersymmetry (Section 3), studies of the dynamics of W-bosons (Section 4), extra dimensions (Section 5), top quark physics (Section 6), and QCD and hadron physics (Section 7). In concluding we present a short list of processes which appear most important for the physics studies at a photon collider.

2 Study of the Higgs Boson

The study of the Higgs boson plays an essential role in exploring the electroweak symmetry breaking and the origin of mass. The lower bound on M_h from direct searches at LEP is presently 113.5 GeV at 95% confidence level (CL) [32]. A surplus of events at LEP provides tantalizing indications of a Higgs boson with $M_h = 115^{+1.3}_{-0.7}$ GeV (90% CL) [33,32]. Recent global anal-

yses of precision electroweak data [30] suggest that the Higgs boson is light, yielding at 95% CL that $M_h = 62^{+53}_{-30}$ GeV. There is remarkable agreement with the well known upper bound of ~ 130 GeV for the lightest Higgs boson mass in the minimal version of supersymmetric theories [34]. Such a Higgs boson should definitely be discovered at the LHC if not already at the TEVATRON.

Once the Higgs boson is discovered, it will be crucial to determine the mass, the total width, spin, parity, CP–nature and the tree–level and one–loop induced couplings in a model–independent way. Here the e^+e^- and $\gamma\gamma$ modes of the LC will play a central role. The $\gamma\gamma$ collider option of an LC offers the unique possibility to produce the Higgs boson as an s–channel resonance [35–37]:

$$\gamma\gamma \to h_0 \to b\bar{b}, WW^*, ZZ, \tau\tau, gg, \gamma\gamma \ \ldots \ .$$

The total width of the Higgs boson at masses below 400 GeV is much smaller than the characteristic width of the $\gamma\gamma$ luminosity spectra (FWHM $\sim$ 10–15%), so that the Higgs production rate is proportional to $dL_{\gamma\gamma}/dW_{\gamma\gamma}$:

$$\dot{N}_{\gamma\gamma \to h} = L_{\gamma\gamma} \times \frac{dL_{\gamma\gamma} M_h}{dW_{\gamma\gamma} L_{\gamma\gamma}} \frac{4\pi^2 \Gamma_{\gamma\gamma}(1 + \lambda_1\lambda_2)}{M_h^3} \equiv L_{\gamma\gamma} \times \sigma^{eff}. \qquad (3)$$

where λ_i are the photon helicities. The Higgs search and study can be done best by exploiting the high energy peak of the $\gamma\gamma$ luminosity spectrum where $dL_{\gamma\gamma}/dW_{\gamma\gamma}$ has a maximum and the photons have a high degree of circular polarization. The effective cross section for $(dL_{\gamma\gamma}/dW_{\gamma\gamma})(M_h/L_{\gamma\gamma}) = 7$ and $1 + \lambda_1\lambda_2 = 2$ is presented in Fig. 4. The luminosity in the high energy luminosity peak ($z > 0.8 z_m$) was defined in Section 1. For the luminosities given in Table 1, the ratio of the Higgs rates in $\gamma\gamma$ and e^+e^- collisions is about 1 to 5 for $M_h = 100$–200 GeV.

The Higgs boson at photon colliders can be detected as a peak in the invariant mass distribution or (and) can be searched for by energy scanning using the sharp high energy edge of the luminosity distribution [18,38]. The scanning allows also to control backgrounds. A cut on the acollinearity angle between two jets from the Higgs decay ($bb, \tau\tau$, for instance) allows to select events with a narrow distribution (FWHM $\sim$ 8%) on the invariant mass [39,19].

The $\gamma\gamma$ partial width $\Gamma(h \to \gamma\gamma)$ of the Higgs boson is of special interest, since it is generated at the one–loop level including all heavy charged particles with masses generated by the Higgs mechanism. In this case the heavy particles do not decouple. As a result, the Higgs cross section in $\gamma\gamma$ collisions is sensitive to contributions of such particles with masses beyond the energy covered directly by the accelerators.

Due to the high cross section some Higgs branching ratios can be measured in $\gamma\gamma$ collisions with accuracies comparable or even better than those in e^+e^-

collisions. Combined measurements of $\Gamma(h \to \gamma\gamma)$ and $\mathrm{BR}(h \to \gamma\gamma)$ at the e^+e^- and $\gamma\gamma$ LC provide a model independent measurement of the total Higgs width [40].

The required accuracy of the $\Gamma(h \to \gamma\gamma)$ measurements in the SUSY sector can be inferred from the results of the studies of the coupling of the lightest SUSY Higgs boson to two photons in the decoupling regime [41]. It was shown that in the decoupling limit, where all other Higgs bosons and the supersymmetric particles are very heavy, chargino and top squark loops can generate a sizable difference between the standard and the SUSY two–photon Higgs couplings. Typical deviations are at the level of a few percent. Top squarks heavier than 250 GeV can induce deviations larger than $\sim 10\%$ if their couplings to the Higgs boson are large.

The control of the polarizations of back-scattered photons provides a powerful tool for exploring the CP properties of any single neutral Higgs boson that can be produced with reasonable rate at the photon collider [42–44]. CP-even Higgs bosons h^0, H^0 couple to the combination $\vec{\varepsilon_1}\cdot\vec{\varepsilon_2}$, while the CP-odd Higgs boson A^0 couples to $[\vec{\varepsilon}_1 \times \vec{\varepsilon}_2]\cdot\vec{k_\gamma}$, where $\vec{\varepsilon}_i$ are photon polarization vectors. The scalar Higgs boson couples to linearly polarized photons with a maximal strength if the polarization vectors are parallel, the pseudoscalar Higgs boson if the polarization vectors are perpendicular:

$$\sigma \propto 1 \pm l_{\gamma 1} l_{\gamma 2} \cos 2\phi, \tag{4}$$

$l_{\gamma i}$ are the degrees of linear polarization and ϕ is the angle between $\vec{l}_{\gamma 1}$ and $\vec{l}_{\gamma 2}$. The signs $\pm$ correspond to the CP$= \pm 1$ scalar particles.

2.1 Light $\mathcal{SM}$ or $\mathcal{MSSM}$ Higgs Boson

A light Higgs boson h with mass below the WW threshold can be detected in the $b\bar{b}$ decay mode. Simulations of this process have been performed in Refs. [37,46,20,47,48,45]. The main background to the $h \to b\bar{b}$ is the continuum production of $b\bar{b}$ and $c\bar{c}$ pairs. A high degree of circular polarization of the photon beams is crucial in this case, since for equal photon helicities ($\pm\pm$), which relevant for the spin–zero resonant states, the $\gamma\gamma \to q\bar{q}$ QED Born cross section is suppressed by a factor $m_q^2/W_{\gamma\gamma}^2$ [35,49]. Another potentially dangerous background originates from heavy quark pair production accompanied by the radiation of an additional gluon, which is not suppressed even for the equal photon helicities [50,51]. In addition, virtual QCD corrections for $J_z = 0$ were found to be especially large due to a double-logarithmic enhancement factor, so that the corrections are comparable or even larger than the Born contribution for the two-jet final topologies [50]. Recent studies on Higgs production

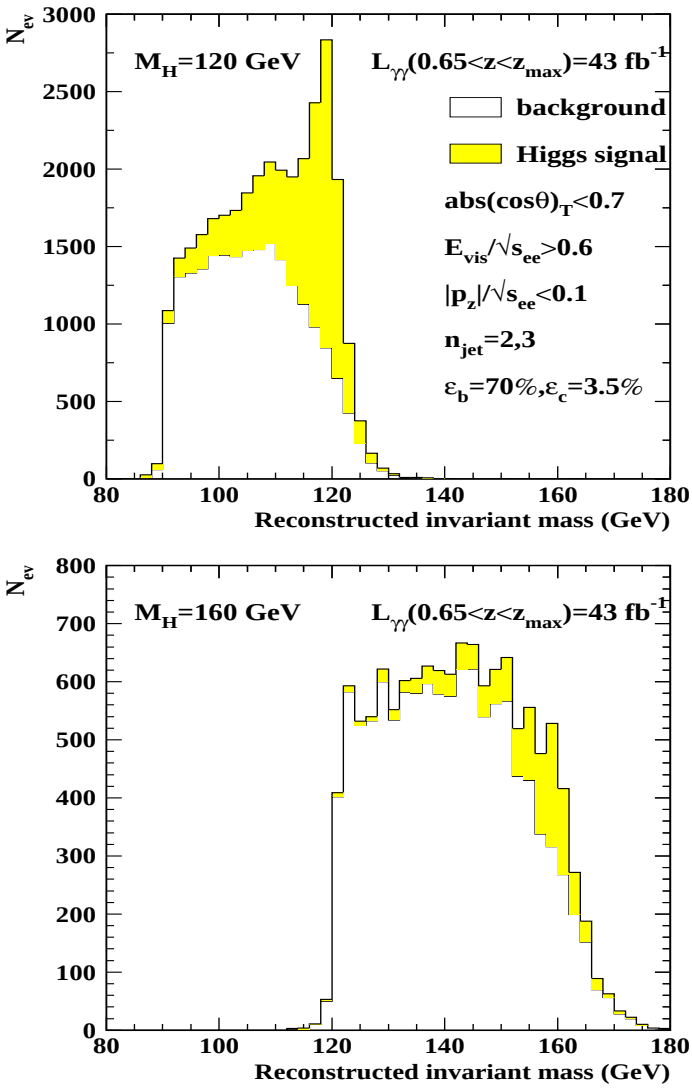

Fig. 5. Mass distributions for the Higgs signal and heavy quark background for a) $M_{\rm h} = 120$ GeV and b) 160 GeV [45].

at photon colliders [45,52,48] include gluon emission in $\gamma\gamma \to q\bar{q}$ and all next-to-leading QCD corrections, as well as resummed leading double-logarithmic corrections [53,54].

A Monte Carlo simulation of $\gamma\gamma \to h \to b\bar{b}$ for $M_h = 120$ and 160 GeV has been performed for an integrated luminosity in the high energy peak of $L_{\gamma\gamma}(0.8z_m < z < z_m) = 43$ fb^{-1} in Ref. [45,52]. Real and virtual gluon corrections for the Higgs signal and the backgrounds [50,51,54,52,48] have been taken into account.

The results for the invariant mass distributions for the combined $b\bar{b}(\gamma)$ and $c\bar{c}(\gamma)$ backgrounds, after cuts, and for the Higgs signal are shown in in Fig. 5 [45]. Due to the large charm production cross-section in $\gamma\gamma$ collisions, excellent b tagging is required [45,48]. A b tagging efficiency of 70% for $\bar{b}b$ events and

residual efficiency of 3.5% for $\bar{c}c$ events were used in these studies.

For a $\gamma\gamma$ luminosity in the high energy peak of 43 fb^{-1} a relative statistical error of

$$\frac{\Delta[\Gamma(h \to \gamma\gamma)\mathrm{BR}(h \to b\bar{b})]}{[\Gamma(h \to \gamma\gamma)\mathrm{BR}(h \to b\bar{b})]} \approx 2\% \tag{5}$$

can be achieved in the Higgs mass range between 120 and 140 GeV.

The statistical accuracy decreases for $M_h > 140$ GeV where the WW^* decay mode becomes important and $b\bar{b}$ is not the dominant decay mode any more. For $M_h = 160$ GeV the statistical error is about 8%.

Assuming that the $h \to b\bar{b}$ branching ratio $\mathrm{BR}(h \to b\bar{b})$ can be measured at the LC in e^+e^- (and $\gamma\gamma$) collisions with an accuracy of 1% [55] the partial two-photon Higgs width can be calculated using the relation

$$\Gamma(h \to \gamma\gamma) = \frac{[\Gamma(h \to \gamma\gamma)\mathrm{BR}(h \to b\bar{b})]}{[\mathrm{BR}(h \to b\bar{b})]} \tag{6}$$

with almost the same accuracy as in Eq.(5). Such a high precision of the $\Gamma(h \to \gamma\gamma)$ measurement can only be achieved at the $\gamma\gamma$ mode of the LC. With such an accuracy it will be possible to discriminate between the $\mathcal{SM}$ Higgs particle and the lightest scalar Higgs boson of the $\mathcal{MSSM}$ or $2\mathcal{HDM}$ [41] and to isolate contributions of new heavy particles.

The $\mathcal{SM}$ Higgs boson with mass $135 < M_h < 190$ GeV will predominantly decay into WW^* or WW pairs. This decay mode should permit the detection of the Higgs signal below and slightly above the threshold of WW pair production [56]. In order to determine the two-photon Higgs width in this case the relation

$$\Gamma(h \to \gamma\gamma) = \frac{[\Gamma(h \to \gamma\gamma)\mathrm{BR}(h \to WW^*)]}{[\mathrm{BR}(h \to WW^*)]}, \tag{7}$$

can be used, where $\mathrm{BR}(WW^*)$ is obtained from the measurements of $\sigma(e^+e^- \to hZ) \times \mathrm{BR}(WW^*)$ and $\sigma(e^+e^- \to hZ)$. For $M_h = 160$ GeV the product $\Gamma(h \to \gamma\gamma)\mathrm{BR}(h \to WW^*)$ can be measured at the photon collider with the statistical accuracy better than 2% for an integrated $\gamma\gamma$ luminosity of 40 fb^{-1} in the high energy peak. The accuracy of $\Gamma(h \to \gamma\gamma)$ will be determined by the accuracy of $\mathrm{BR}(h \to WW^*)$ in e^+e^- experiments, expected to be about 2%.

Above the ZZ threshold, the most promising channel to detect the Higgs

signal is the reaction $\gamma\gamma \to ZZ$ [57]. In order to suppress the huge background from the tree level W^+W^- pair production leptonic ($l^+l^-\ l^+l^-$, $BR = 1\%$) or semileptonic ($l^+l^-\ q\bar{q}$, $BR = 14\%$) decay modes of the ZZ pairs must be selected. Although there is only a one-loop induced continuum production of ZZ pairs in the $\mathcal{SM}$, a large irreducible background to the Higgs signal well above the WW threshold is generated in the continuum [57]. Due to this background the intermediate mass Higgs boson signal can be observed at the $\gamma\gamma$ collider in the ZZ mode only if the Higgs mass is less than 350–400 GeV.

Hence, the two-photon $\mathcal{SM}$ Higgs width can be measured at the photon collider, either in $b\bar{b}$, $WW(WW^*)$ or $ZZ(ZZ^*)$ decay modes, up to the Higgs mass of 350–400 GeV. Other decay modes, like $h \to \tau\tau, \gamma\gamma$, can also be explored at photon colliders, but no studies have been carried out so far.

Assuming that in addition to the measurement of the $h \to b\bar{b}$ branching ratio also the BR($h \to \gamma\gamma$) can be measured at the e^+e^- linear collider with an accuracy [58] 10–15%, the total width of the Higgs boson can be determined in a model independent way

$$\Gamma_h = \frac{[\Gamma(h \to \gamma\gamma)\mathrm{BR}(h \to b\bar{b})]}{[\mathrm{BR}(h \to \gamma\gamma)][\mathrm{BR}(h \to b\bar{b})]} \tag{8}$$

to an accuracy dominated by the expected error on BR($h \to \gamma\gamma$). The measurement of this branching ratio at the photon collider can improve the accuracy of the total Higgs width.

The total Higgs width can also be determined in the e^+e^- collisions using the reaction $e^+e^- \to h\nu\bar{\nu}$, in which the Higgs boson is produced in collisions of virtual W bosons, $\sigma \propto \Gamma(h \to WW^*)$. Combined with the measurement of BR(WW^*) in e^+e^- collisions the total Higgs width can be determined in this way [59,60]. The typical precision of such a measurement for a Higgs mass range of 110–140 GeV is about $(10 - 3)\%$.

2.2 Heavy $\mathcal{MSSM}$ Higgs Bosons

The minimal supersymmetric extension of the Standard Model includes two charged ($H^\pm$) Higgs bosons and three neutral Higgs bosons: the light CP-even Higgs particle (h), the heavy CP-even (H) and the CP-odd (A) Higgs states. For large value of the A mass, the properties of the light CP-even Higgs boson h are similar to the light $\mathcal{SM}$ Higgs boson, and it can be detected in the $b\overline{b}$ decay mode, just as the $\mathcal{SM}$ Higgs boson. Its mass is limited to $M_h \lesssim 130$ GeV. However, the masses of the heavy Higgs bosons $H, A, H^\pm$ are expected to be of the order of the electroweak scale up to about one TeV. They are nearly

degenerate. The WW and ZZ decay modes are suppressed for H, and these decays are forbidden for A. Instead of the WW, ZZ decay modes, the $t\bar{t}$ decay channel may be useful, if the Higgs boson masses are heavier than $2M_t$ and if $\tan\beta \ll 10$. An important property of the SUSY couplings is the enhancement of the bottom Yukawa couplings with increasing $\tan\beta$. For moderate and large values of $\tan\beta$, the decay mode to $b\bar{b}$ and to $\tau^+\tau^-$ is substantial [61,62].

Extensive studies have demonstrated that, while the light Higgs boson h of the $\mathcal{MSSM}$ can be found at the LHC, the heavy bosons H and A may escape the discovery for intermediate values of $\tan\beta$ [63]. At an e^+e^- LC heavy $\mathcal{MSSM}$ Higgs bosons can only be found in associated production, $e^+e^- \to HA$ [64], with H and A having almost equal masses. In the first phase of the LC collider with a total e^+e^- energy of 500 GeV, the heavy Higgs bosons can thus be discovered for a mass up to about 250 GeV. To extend the mass reach by a factor of 1.6, the $\gamma\gamma$ option of LC can be used, where these bosons can be produced singly.

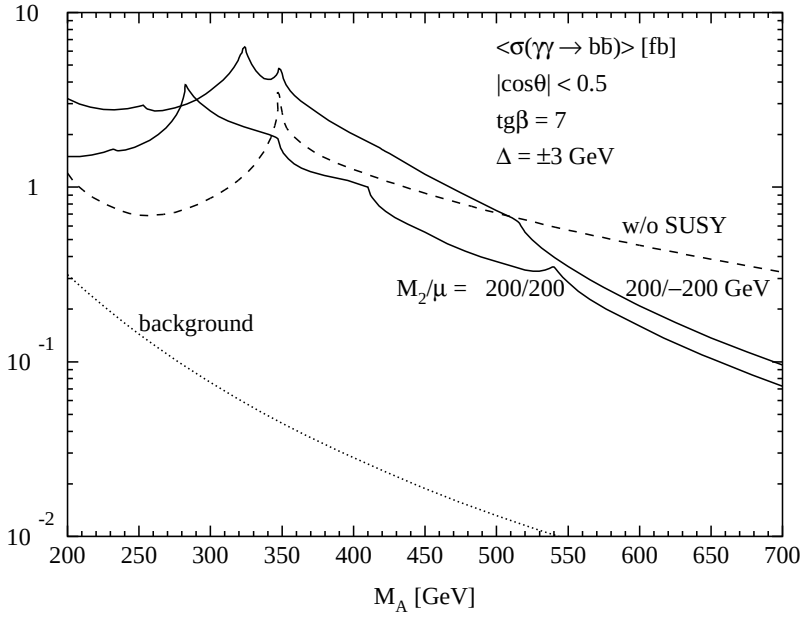

Fig. 6. (a) Cross section for resonant heavy Higgs H, A boson production as a function of the pseudoscalar Higgs mass M_A with decay into $b\bar{b}$ pairs, and the corresponding background cross section. The maximum of the photon luminosity has been turned to M_A. Cuts as indicated. The $\mathcal{MSSM}$ paraameters have been chosen as $\tan\beta = 7, M_2 = \pm\mu = 200$ GeV; the limit of vanishing SUSY-particle contributions is shown for comparison. The cross sections are defined in $b\bar{b}$ mass bins of $M_A \pm 3$ GeV around the maximum of the $\gamma\gamma$ luminosity. See also comments in text.

The results for the cross section of the H, A signal in the $b\bar{b}$ decay mode and the corresponding background for the value of $\tan\beta = 7$ are shown in Fig. 6 as a

function of the pseudoscalar mass M_A [61]. From the figure one can see that the background is strongly suppressed with respect to the signal. The significance of the heavy boson signals is sufficient for a discovery of the Higgs particles with masses up to about 70–80% of the e^+e^- c.m.s. energy. For a 500 GeV e^+e^- LC the H, A bosons with masses up to about 400 GeV can be discovered in the $b\bar{b}$ channel. For a LC with $\sqrt{s_{ee}} = 900$ GeV the range can be extended to about 700 GeV [62,65]. For heavier Higgs masses the signal becomes too small to be detected. Note that the cross section given in Fig.6 is related to the luminosity $k^2 L_{geom} \sim 0.4 L_{geom}$ which is $4.8 \times 10^{34}\mathrm{cm}^{-2}\mathrm{s}^{-1} (\sim 1.5 L_{e^+e^-})$ for 2E = 500 GeV and it grows proportional to the energy.

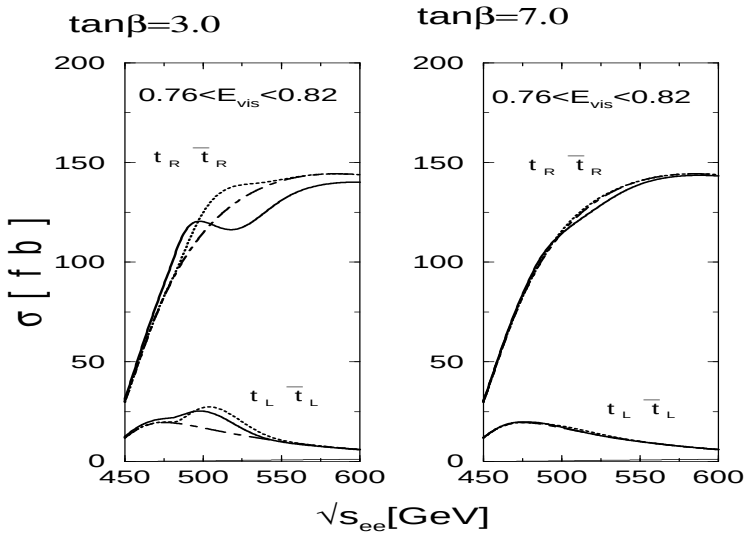

Fig. 7. The effective top pair cross sections convoluted with the $\gamma\gamma$ luminosity within the visible energy range as indicated. The bold-solid curves correspond to the correct cross sections, the dotted curves are the ones neglecting the interference, and the dot-dashed are the continuum cross sections, respectively. The upper curves are for $t_R\bar{t}_R$, and the lower ones for $t_L\bar{t}_L$. The sum of the tree cross sections for $t_R\bar{t}_L$ and $t_L\bar{t}_R$, are also plotted in the thin-solid line located very near to the bottom horizontal axis. The left figure is for $\tan\beta = 3$, and the right for $\tan\beta = 7$ [66].

The almost degenerate H and A states can be separated by using the linear polarization of the colliding photons (see eq.4). The H and A states can be produced from collisions of parallel and perpendicularly polarized incoming photons, respectively [67,42,44,43,68]. Next-to-leading order QCD corrections to the asymmetry of heavy quark production in linearly polarized photon beams are shown to be small [69]. The possible CP-violating mixing of H and A can be distinguished from the overlap of these resonances by studying the polarization asymmetry in the two-photon production [70].

The interference between H and A states can be also studied in the reaction $\gamma\gamma \to t\bar{t}$ with circularly polarized photon beams by measuring the top quark helicity [66]. The corresponding cross sections are shown in Fig. 7. The effect of

the interference is clearly visible for the value $\tan\beta = 3$. The RR cross section is bigger than the LL cross section [$R(L)$ denotes the right(left) helicity] due to the continuum. Large interference effects are visible in both modes. Without the measurement of the top quark polarization there still remains a strong interference effect between the continuum and the Higgs amplitudes, which can be measured.

For the pair production of charged Higgses $\gamma\gamma \to H^+H^-$, due to much larger cross section, Fig.3, the event rate at the photon collider will be almost an order of magnitude larger than at the e^+e^- LC.

2.3 Extended Higgs Models

The scenario, in which all new particles are very heavy, can be realized not only in the $\mathcal{MSSM}$ but also in other extended models of the $\mathcal{SM}$ Higgs sector, for example in models with two Higgs doublets. In this case the two-photon Higgs boson width differs from the $\mathcal{SM}$ value due to contributions of extra heavy charged particles, i.e. charged Higgs bosons in the $2\mathcal{HDM}$.

Different models for the $2\mathcal{HDM}$ have been discussed in Ref. [71]. Assuming that the branching ratios of the observed Higgs boson to quarks, Z or W bosons are close to their $\mathcal{SM}$ values, two sets of possible values for the couplings are obtained. For solution A all these couplings are close to their values in the $\mathcal{SM}$ up to a common sign. For solution B absolute values of the couplings are close to their $\mathcal{SM}$ values, but the coupling to quark $q = u(t)$ or $d(b)$ is of opposite sign as compared to the coupling to the gauge bosons. Fig. 8 shows deviations of the two-photon Higgs width from the $\mathcal{SM}$ value for these two solutions. The shaded regions are derived from the anticipated 1σ experimental bounds around the $\mathcal{SM}$ values for the Higgs couplings to fermions and gauge bosons. Comparing the numbers in these figures with the accuracy of the two-photon Higgs width at a photon collider, it can concluded that the difference between $\mathcal{SM}$ and $2\mathcal{HDM}$ should definitely be observed [71].

The CP parity of the neutral Higgs boson can be measured using linearly polarized photons. Moreover, if the Higgs boson is a mixture of CP-even and CP-odd states, as in a general $2\mathcal{HDM}$ with CP-violating neutral sector, the interference of these two terms gives rise to a CP-violating asymmetries [42–44,72,70]. Two CP-violating ratios could contribute to linear order with respect to CP-violating couplings:

$$\mathcal{A}_1 = \frac{|\mathcal{M}_{++}|^2 - |\mathcal{M}_{--}|^2}{|\mathcal{M}_{++}|^2 + |\mathcal{M}_{--}|^2}, \quad \mathcal{A}_2 = \frac{2Im(\mathcal{M}^*_{--}\mathcal{M}_{++})}{|\mathcal{M}_{++}|^2 + |\mathcal{M}_{--}|^2}. \tag{9}$$

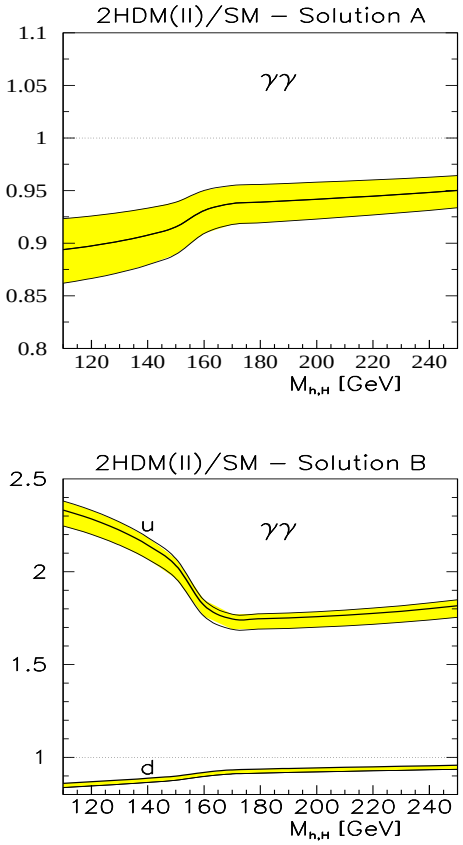

Fig. 8. The ratio of the two-photon Higgs width in the $2\mathcal{HDM}$ to its $\mathcal{SM}$ value, for two different solutions [71]. See also the text.

Since the event rate for Higgs boson production in $\gamma\gamma$ collisions is given by

$$dN = dL_{\gamma\gamma} dPS \frac{1}{4}(|\mathcal{M}_{++}|^2 + |\mathcal{M}_{--}|^2) \times[(1 + \langle\xi_2\tilde{\xi}_2\rangle) + (\langle\xi_2\rangle + \langle\tilde{\xi}_2\rangle)\mathcal{A}_1 + (\langle\xi_3\tilde{\xi}_1\rangle + \langle\xi_1\tilde{\xi}_3\rangle)\mathcal{A}_2], \quad (10)$$

where ξ_i, $\tilde{\xi}_i$ are the Stokes polarization parameters, two CP-violating asymmetries can be observed. The asymmetry measured with circularly polarized photons is given by

$$T_- = \frac{N_{++} - N_{--}}{N_{++} + N_{--}} = \frac{\langle\xi_2\rangle + \langle\tilde{\xi}_2\rangle}{1 + \langle\xi_2\tilde{\xi}_2\rangle}\mathcal{A}_1, \quad (11)$$

where $N_{\pm\pm}$ correspond to the event rates for positive (negative) initial photon helicities. Experimentally the asymmetry is measured by simultaneously flipping the helicities of the laser beams used for production of polarized electrons and $\gamma \to e$ conversion. The asymmetry measured with linearly polarized

photons is given by

$$T_\psi = \frac{N(\phi = \frac{\pi}{4}) - N(\phi = -\frac{\pi}{4})}{N(\phi = \frac{\pi}{4}) + N(\phi = -\frac{\pi}{4})} = \frac{\langle \xi_3 \tilde{\xi}_1 \rangle + \langle \xi_1 \tilde{\xi}_3 \rangle}{1 + \langle \xi_2 \tilde{\xi}_2 \rangle} \mathcal{A}_2, \tag{12}$$

where ϕ is the angle between the linear polarization vectors of the photons. The asymmetries are typically larger than 10% [42–44,72,70] and they are observable for a large range of $2\mathcal{HDM}$ parameter space if CP violation is present in the Higgs potential.

Hence, a high degree of both circular and linear polarizations for the high energy photon beams gives additional opportunities at the $\gamma\gamma$ collider for the detailed study of the Higgs sector.

3 Supersymmetry

In $\gamma\gamma$ collisions, any kind of the charged particles can be produced in pairs if the mass is below the kinematical bound. Important cases for a photon collider are the charged sfermions [20,73], the charginos [20,74] and the charged Higgs bosons.

For the $\gamma\gamma$ luminosities given in the Table 1, the production rates for these particles will be larger than in e^+e^- collisions. Hence detailed studies of charged supersymmetric particles are possible at the $\gamma\gamma$ collider. In addition, the cross sections in $\gamma\gamma$ collisions are given by pure QED to leading order, while in e^+e^- collisions also Z-boson and sometimes t-channel exchanges contribute. So, studies of these production processes in both channels provide complementary information about the interactions of these charged sparticles.

The $e\gamma$ collider could be the ideal machine for the discovery of the scalar electron and neutralino in the reaction $e^-\gamma \to \tilde{e}^-\tilde{\chi}_1^0$ [20,75–77]. They could be discovered in γe collisions up to the kinematical limit of

$$M_{\tilde{e}^-} < 0.9\sqrt{s}_{ee} - M_{\tilde{\chi}_1^0}, \tag{13}$$

where $\sqrt{s_{ee}}$ is the energy of the original e^+e^- collider. This bound would exceed the bound for $\tilde{e}^+\tilde{e}^-$ pair production in e^+e^- collisions if $M_{\tilde{\chi}_1^0} < 0.4\sqrt{s}_{ee}$. [4]

In some scenarios of supersymmetric extensions of the Standard Model stoponium bound states $\tilde{t}\bar{\tilde{t}}$ are formed. A photon collider would be the ideal machine

[4] Cross sections of the reactions $e^+e^- \to \tilde{e}^\mp\tilde{\chi}_1^0 e^\pm$ with lower threshold in e^+e^- collisions are suppressed by an extra factor of α.

for the discovery and study of these new narrow strong resonances [78]. About ten thousand stoponium resonances for $M_S = 200$ GeV will be produced for an integrated $\gamma\gamma$ luminosity in the high energy peak of 100 fb^{-1}. Thus precise measurements of the stoponium effective couplings, mass and width should be possible. At e^+e^- colliders the counting rate will be much lower and in some scenarios the stoponium cannot be detected due to the large background [78].

4 W Boson Interactions

One of the best known examples of new physics scenarios which clearly show the complementarity of the e^+e^- and the $\gamma\gamma$, γe modes of an LC, are anomalous gauge couplings of the W boson. Recent experiments at LEP2 and the Tevatron have observed WW, ZZ pair production and they have verified that the cross sections for the production of weak gauge boson pairs, at least in the region close to threshold, conform to the Standard Model predictions. New strong interactions that might be responsible for the electroweak symmetry breaking can affect the triple and quartic couplings of the weak vector bosons. The precision measurements of these couplings, as well as corresponding effects on the top quark couplings can provide clues to the mechanism of the electroweak symmetry breaking. Moreover, if all new particles are very heavy, anomalous couplings are an important source of information on the mechanism of EWSB. Estimates suggest that a high level of precision is needed, which is much higher than the current bounds close to 10^{-1} on the parameters of the W vertices from LEP2 and the Tevatron [79]. Due to the huge cross sections, of the order of 10^2 pb, well above the thresholds, the $\gamma\gamma \to W^+W^-$ and $e^-\gamma \to \nu W^-$ processes seem to be ideal reactions to study the anomalous gauge interactions.

4.1 Anomalous Gauge Boson Couplings

The relevant process at the e^+e^- collider is $e^+e^- \to W^+W^-$. This reaction is dominated by the large t-channel neutrino exchange diagram which however can be removed using electron beam polarization. The cross section of W^+W^- pair production in e^+e^- collisions with right-handed electron beams, eliminating the neutrino exchange, has a maximum of about 2 pb at LEP2 and decreases at higher energy.

The two main processes at the photon collider are $\gamma\gamma \to W^+W^-$, $e\gamma \to W\nu$. Their total cross sections for center–of–mass energies above 200 GeV are about 80 pb and 40 pb, respectively, and they do not decrease with energy. Hence the W production cross sections at the photon collider are at least 20–40 times

larger than the cross section at the e^+e^- collider. This enhancement makes event rates at the photon collider one order of magnitude larger than at an e^+e^- collider, even when the lower $\gamma\gamma$, γe luminosities are taken into account. Specifically for the integrated $\gamma\gamma$ luminosity of 100 fb^{-1}, about 8×10^6 W^+W^- pairs are produced at the photon collider. Note that while $\gamma e \to W\nu$ and $\gamma\gamma \to WW$ isolate the anomalous photon couplings to the W, $e^+e^- \to WW$ involves potentially anomalous Z couplings so that the two LC modes are complementary with each other.

While there have been extensive analyses [80] of anomalous triple gauge boson couplings at e^+e^- colliders, the corresponding processes $\gamma e \to W\nu$ and $\gamma\gamma \to WW$ have generally received less attention in the literature [81,82,20] and the higher order processes were not considered in detail.

The analysis of $\gamma\gamma \to WW$ has been performed in Refs. [20,83] with the detector simulation. The analysis at photon colliders is compared to that at e^+e^- colliders. The results have been obtained only from analyses of the total cross section. With the W decay properties taken into account further improvements can be expected. The resulting accuracy on λ_γ is comparable with e^+e^- analyses, while a similar accuracy on $\delta\kappa_\gamma$ can be achieved at 1/20–th of the e^+e^- luminosity.

In addition, the process $e\gamma \to W\nu$ which has a large cross section, is very sensitive to the admixture of right–handed currents in the W couplings with fermions: $\sigma_{e\gamma \to W\nu} \propto (1-2\lambda_e)$.

Many processes of 3rd and 4th order have quite large cross sections [84–87] at the photon collider:

$$\begin{aligned} e\gamma &\to eWW & \gamma\gamma &\to ZWW \\ e\gamma &\to \nu WZ & \gamma\gamma &\to WWWW \\ & & \gamma\gamma &\to WWZZ \end{aligned}$$

It should also be noted, that in $\gamma\gamma$ collisions the anomalous $\gamma\gamma W^+W^-$ quartic couplings can be probed. However, the higher event rate does not necessarily provide better bounds on anomalous couplings. In some models electroweak symmetry breaking leads to large deviations mainly in longitudinal W_LW_L pair production [82]. On the other hand the large cross section of the reaction $\gamma\gamma \to W^+W^-$ is due to transverse W_TW_T pair production. In such a case transverse W_TW_T pair production would represent a background for the longitudinal W_LW_L production. The relative yield of W_LW_L can be considerably improved after a cut on the W scattering angle. Asymptotically for $s_{\gamma\gamma} \gg M_W^2$ the production of W_LW_L is as much as 5 times larger than at a e^+e^- LC.

However, if anomalous couplings manifest themselves in transverse W_TW_T pair production, e.g. in theories with large extra dimensions, then the interference with the large $\mathcal{SM}$ transverse contribution is of big advantage in the photon collider.

4.2 Strong $WW \to WW$, $WW \to ZZ$ Scattering

If a strong-coupling EWSB breaking scenario is realized in Nature, W and Z bosons will interact strongly at high energy. For example, if no Higgs boson exists with a mass below 1 TeV, the longitudinal components of the electroweak gauge bosons must become strongly interacting at energies above 1 TeV to comply with the requirements of unitarity for the W_LW_L, Z_LZ_L scattering amplitudes. In such scenarios novel resonances can be formed in the $\mathcal{O}$(1 TeV) energy range which can be produced in W_LW_L collisions. In these scenarios, W_LW_L must be studied at energies of the order of 1 TeV. In e^+e^- collisions W_LW_L scattering can be investigated by using W bosons radiated off the electron and positron beams in the reaction $e^+e^- \to \nu\nu W^+W^-$. If the energy of the $\gamma\gamma$ collisions is high enough, the effective W luminosity in $\gamma\gamma$ collisions becomes large enough to allow for the study of $W^+W^- \to W^+W^-$, ZZ scattering in the reactions

$$\gamma\gamma \to WWWW, \;\; WWZZ. \tag{14}$$

Each incoming photon turns into a virtual WW pair, followed by the scattering of one W from each such pair to form the final WW or ZZ pairs [88–91]. The same reactions can be used to study anomalous quartic $WWWW$, $WWZZ$ couplings.

A potential advantage of the $\gamma\gamma$ collider is the longitudinal W spectrum inside the photon [92]. Due to the hard component, with the logarithmic enhancement factor, the distribution function at large z is bigger for photons than for electrons. For $\sqrt{s} = 1$ TeV the W_LW_L luminosity distributions in $\gamma\gamma$ and e^+e^- collisions are very similar, but $\mathcal{L}_{W_LW_L/\gamma\gamma}$ is larger than $\mathcal{L}_{W_LW_L/e^+e^-}$ by a factor of 5 [90] for $\sqrt{s} = 5$ TeV. A detailed comparison can be carried out only after accurate simulations of the processes have been performed, taken backgrounds into account properly.

5 Extra Dimensions

New ideas have recently been proposed to explain the weakness of the gravitational force [93]. The Minkowski world is extended by extra space dimensions

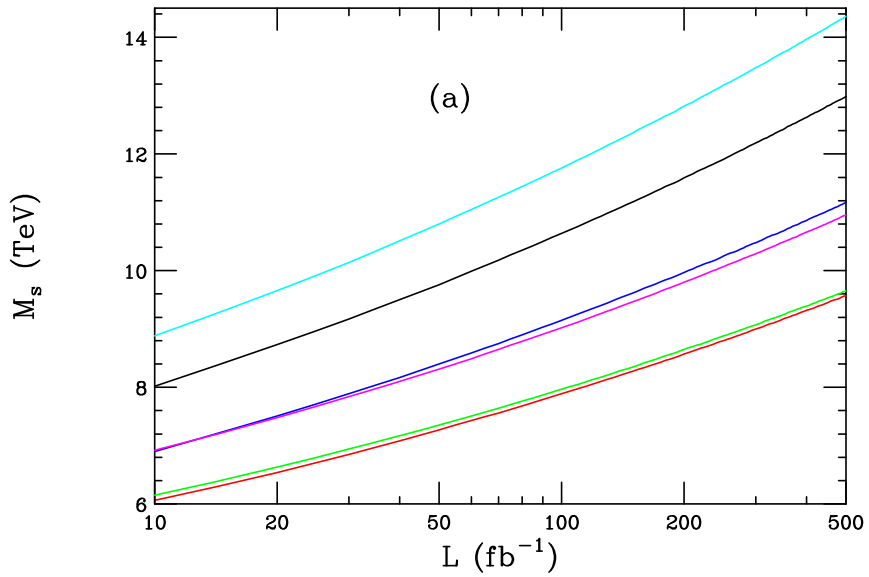

Fig. 9. M_s discovery reach for the process $\gamma\gamma \to W^+W^-$ at a $2E_0 = 1$ TeV LC as a function of the integrated luminosity for the different initial state polarizations assuming $\lambda = 1$. From top to bottom on the right hand side of the figure the polarizations are $(- + +-)$, $(+ - --)$, $(+ + --)$, $(+ - +-)$, $(+ - --)$, and $(+ + ++)$.

which are curled up at small dimensions R. While the gauge and matter fields are confined in the (3+1) dimensional world, gravity propagates through the extended 4+n dimensional world. While the effective gravity scale, the Planck scale, in four dimensions is very large, the fundamental Planck scale in 4+n dimensions may be as low as a few TeV so that gravity may become strong already at energies of the present or next generation of colliders.

Towers of Kaluza–Klein graviton excitations will be realized on the compactified 4+n dimensional space. Exchanging these KK excitations between $\mathcal{SM}$ particles in high–energy scattering experiments will generate effective contact interactions, carrying spin=2 and characterized by a scale M_s of order few TeV. They will give rise to substantial deviations from the predictions of the Standard Model for the cross sections and angular distributions for various beam polarizations [94,95].

Of the many processes examined so far, $\gamma\gamma \to WW$ provides the largest reach for M_s for a given center of mass energy of the LC [96,95]. The main reasons are that the WW final state offers many observables which are particularly sensitive to the initial electron and laser polarizations and the very high statistics due to the 80 pb cross section.

By performing a combined fit to the total cross sections and angular distributions for various initial state polarization choices and the polarization asymmetries, the discovery reach for M_s can be estimated as a function of the

total $\gamma\gamma$ integrated luminosity. This is shown in Fig. 9 [95]. The reach is in the range of $M_s \sim (11\text{–}13) \cdot 2E_0$, which is larger than that obtained from all other processes examined so far. By comparison, a combined analysis of the processes $e^+e^- \to f\bar{f}$ with the same integrated luminosity leads to a reach of only $(6\text{–}7) \cdot 2E_0$.

Other final states in $\gamma\gamma$ collisions are also sensitive to graviton exchanges, two examples being the $\gamma\gamma$ [97,98] and ZZ [96] final states, which however result in smaller search reaches.

6 Studies of the Top Quark

The top quark is heavy and up to now point-like at the same time. The top Yukawa coupling $\lambda_t = 2^{3/4} G_F^{1/2} M_t$ is numerically very close to unity, and it is not clear whether this is related to some deep physical reason. Hence deviations from the $\mathcal{SM}$ predictions should be expected most pronounced in the top sector [99]. Studies of the top quark may shed light on the origin of the mechanism of EWSB. Top quark physics will therefore be a very important part of research programs for all future hadron and lepton colliders. The $\gamma\gamma$ collider is of special interest because of the very clean production mechanism and high rate (review Ref. [100]). Moreover, the S and P partial waves of the final state top quark–antiquark pair produced in $\gamma\gamma$ collisions can be separated by choosing the same or opposite helicities of the colliding photons.

To get a reliable answer for the production cross section near the threshold, it is necessary to resum the Coulombic corrections as for e^+e^- collisions [101]. After resummation, the cross section close to the threshold increases by a factor 4–5 [102]. Recent results [102] show a large difference between the NLO and NNLO predictions.

6.1 Probing Anomalous Couplings in $t\bar{t}$ Pair Production

Two points are different in $\gamma\gamma$ and e^+e^- collisions with respect to the couplings of the top quark:

- in $\gamma\gamma$ collisions the $\gamma t\bar{t}$ coupling enters with the 4th power;
- the $\gamma t\bar{t}$ coupling is isolated in $\gamma\gamma$ collisions while in e^+e^- collisions both $\gamma t\bar{t}$ and $Zt\bar{t}$ couplings contribute.

The effective Lagrangian contains four parameters f_i^α, Ref.[103], where $\alpha = \gamma, Z$; but only couplings with $\alpha = \gamma$ occur in $\gamma\gamma$ collisions. It has been demonstrated [104] that if the cross section can be measured with 2% accuracy, scale

parameters for new physics Λ can be probed up to 10 TeV for $2E_0 = 500$ GeV, with the form factors are taken in the form $f_i^\alpha = (f_i^\alpha)^{SM}(1 + s/\Lambda^2)$. The sensitivity to the anomalous magnetic moment f_2^γ is better in $\gamma\gamma$ than in e^+e^- collisions. The f_4^α term describes the CP violation. The best limit on the imaginary part of the electric dipole moment $Im(f_4^\gamma)$ is about 2.3×10^{-17} $e$cm [105]. It can be derived from the forward-backward asymmetry A_{fb} with initial-beam helicities of electron and laser beams $\lambda_e^1 = \lambda_e^2$ and $\lambda_l^1 = -\lambda_l^2$. The real part of the dipole moment can also be bounded to the order 10^{-17} $e$cm by using linear polarization asymmetries [106].

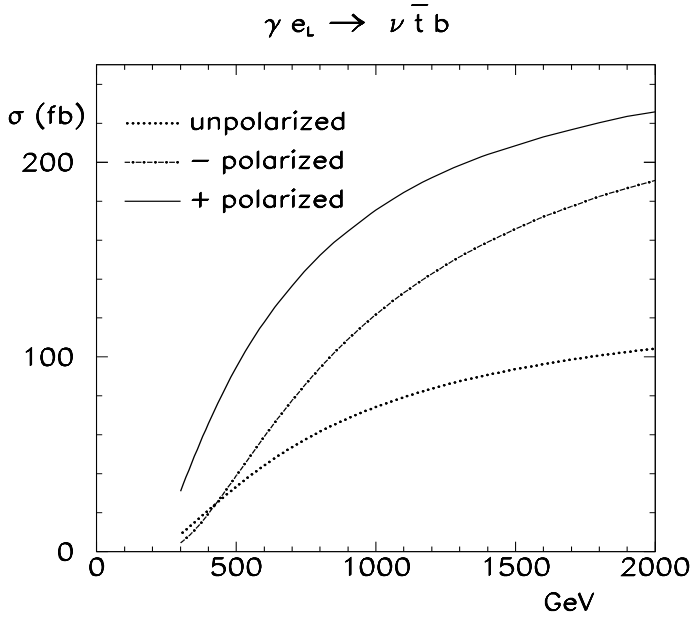

Fig. 10. Single top quark production cross section in γe collisions

6.2 Single Top Production in $\gamma\gamma$ and γe Collisions

Single top production in $\gamma\gamma$ collisions results in the same final state as the top quark pair production [107] and invariant mass cuts are required to suppress direct $t\bar{t}$ contribution. Single top production can also be studied in γe collisions [108]. In contrast to the pair production rate the single top rate is directly proportional to the Wtb coupling and the process is therefore very sensitive to its structure. The anomalous part of the effective Lagrangian, Ref.[103], contains terms $f_{2L(R)} \propto 1/\Lambda$, where Λ is the scale of a new physics.

In the Table 2 [109,110] limits on anomalous couplings from measurements at different machines are shown. The best limits can be reached at very high energy γe colliders, even in the case of unpolarized collisions. In the case of polarized collisions, the production rate increases significantly, cf. Fig. 10 [107],

Table 2
Expected sensitivity for Wtb anomalous couplings measurements. The total integrated luminosity was assumed to be 500 fb^{-1} for e^+e^- collisions and 250 fb^{-1} and 500 fb^{-1} for γe collisions at 500 GeV and 2 TeV, respectively.

	f_2^L	f_2^R
Tevatron ($\Delta_{sys.} \approx 10\%$)	$-0.18 \div +0.55$	$-0.24 \div +0.25$
LHC ($\Delta_{sys.} \approx 5\%$)	$-0.052 \div +0.097$	$-0.12 \div +0.13$
e^+e^- ($\sqrt{s_{e^+e^-}} = 0.5$ TeV)	$-0.025 \div +0.025$	$-0.2 \div +0.2$
γe ($\sqrt{s_{e^+e^-}} = 0.5$ TeV)	$-0.045 \div +0.045$	$-0.045 \div +0.045$
γe ($\sqrt{s_{e^+e^-}} = 2.0$ TeV)	$-0.008 \div +0.035$	$-0.016 \div +0.016$

and the bounds are improved. Only left-handed electrons lead to a nonvanishing cross section.

7 QCD and Hadron Physics

Photon colliders offer a unique possibility to probe QCD in a new unexplored regime. The very high luminosity, the (relatively) sharp spectrum of the backscattered laser photons and their polarization are of great advantage. At the photon collider the following measurements can be performed, for example:

(1) The total cross section for $\gamma\gamma$ fusion to hadrons [111].
(2) Deep inelastic γe $\mathcal{N}C$ and $\mathcal{C}C$ scattering, and measurement of the quark distributions in the photon at large Q^2.
(3) Measurement of the gluon distribution in the photon.
(4) Measurement of the spin dependent structure function $g_1^\gamma(x, Q^2)$ of the photon.
(5) J/Ψ production in $\gamma\gamma$ collisions as a probe of the hard QCD pomeron [112].

$\gamma\gamma$ Fusion to Hadrons

The total cross section for hadron production in $\gamma\gamma$ collisions is a fundamental observable. It provides us with a picture of hadronic fluctuations in photons of high energy which reflect the strong–interaction dynamics as described by quarks and gluons in QCD. Since these dynamical processes involve large distances, predictions, due to the theoretical complexity, cannot be based yet on first principles. Instead, phenomenological models have been developed which

involve elements of ideas which have successfully been applied to the analysis of hadron–hadron scattering, but also elements transferred from pertubative QCD in eikonalized mini–jet models. Differences between hadron–type models and mini–jet models are dramatic in the TESLA energy range. $\gamma\gamma$ scattering experiments are therefore extremely valuable in exploring the dynamics in complex hadronic quantum fluctuations of the simplest gauge particle in Nature.

Deep Inelastic γe Scattering (DIS)

The large c.m. energy in the γe system and the possibility of precise measurement of the kinematical variables x, Q^2 in DIS provide exciting opportunities at a photon collider. In particular it allows precise measurements of the photon structure function(s) with much better accuracy than in the single tagged e^+e^- collisions. The γe collider offers a unique opportunity to probe the photon at low values of x ($x \sim 10^{-4}$) for reasonably large values of $Q^2 \sim 10$ GeV^2 [113]. At very large values of Q^2 the virtual γ exchange in deep inelastic γe scattering is supplemented by significant contributions from Z exchange. Moreover, at very large values of Q^2 the charged–current process becomes effective in deep inelastic scattering, $\gamma e \to \nu X$, which is mediated by virtual W exchange. The study of this process can in particular give information on the flavor decomposition of the quark distributions in the photon [114].

Gluon Distribution in the Photon

The gluon distribution in the photon can be studied in dedicated measurements of the hadronic final state in $\gamma\gamma$ collisions. The following two processes are of particular interest:

(1) Dijet production [115,116], generated by the subprocess $\gamma g \to q\bar{q}$;
(2) Charm production [117], which is sensitive to the mechanism $\gamma g \to c\bar{c}$.

Both these processes, which are at least in certain kinematical regions dominated by the photon–gluon fusion mechanisms, are sensitive to the gluon distribution in the photon. The detailed discussion of these processes have been presented in [118,119].

Spin Dependent Structure Function $g_1^\gamma(x, Q^2)$ of the Photon

Using polarized beams, photon colliders offer the possibility to measure the spin dependent structure function $g_1^\gamma(x, Q^2)$ of the photon [120]. This quantity is completely unknown and its measurement in polarized γe DIS would be

extremely interesting for testing QCD predictions in a broad region of x and Q^2. The high–energy photon colliders allow to probe this quantity for very small values of x [121].

Probing the QCD Pomeron by J/Ψ Production in $\gamma\gamma$ Collisions

The exchange of the hard QCD (or BFKL) pomeron is presumably the dominant mechanism of the process $\gamma\gamma \to J/\psi\, J/\psi$. Theoretical estimates of the cross–section presented in [122] have demonstrated that measurement of the reaction $\gamma\gamma \to J/\psi\, J/\psi$ at the photon collider should be feasible.

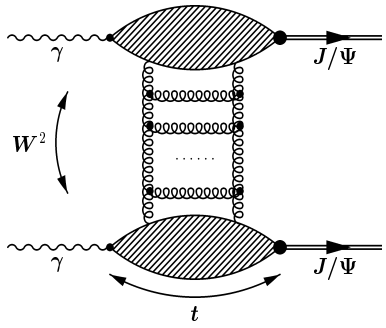

Fig. 11. The QCD Pomeron exchange mechanism of the processes $\gamma\gamma \to J/\psi J/\psi$.

8 Conclusions

A short list of processes which we consider to be most important for the physics program of the photon collider option of the LC, is presented in Table 3.

Of course there exist lots of other possible manifestations of new physics in the $\gamma\gamma$, γe collisions which we have not discussed here. The study of resonant excited electron production $\gamma e \to e^*$, the production of excited fermions $\gamma\gamma \to f^* f$[123,10], leptoquark production $e\gamma \to (eQ)\bar{Q}$ [124], a magnetic monopole signal in the reaction of $\gamma\gamma$ elastic scattering [125] *etc* may be mentioned in this context.

To summarize, the photon collider will allow us to study the physics of EWSB in both the weak-coupling and the strong-coupling scenarios, as well as to search for a rich spectrum of new physics manifestations. Measurements of the two-photon Higgs width of the h, H and A Higgs states provide a strong motivation for developing the technology of the $\gamma\gamma$ collider option. Photon colliders offer unique possibilities for probing the photon structure and the QCD Pomeron. Polarized photon beams, large cross sections and sufficiently large luminosities allow to enhance significantly the discovery limits of many

Table 3
Gold–plated processes at photon colliders.

Reaction	**Remarks**
$\gamma\gamma \to h^0 \to b\bar{b}$	$\mathcal{SM}$ or $\mathcal{MSSM}$ Higgs, $M_{h^0} < 160$ GeV
$\gamma\gamma \to h^0 \to WW(WW^*)$	$\mathcal{SM}$ Higgs, $140\,\mathrm{GeV} < M_{h^0} < 190$ GeV
$\gamma\gamma \to h^0 \to ZZ(ZZ^*)$	$\mathcal{SM}$ Higgs, $180\,\mathrm{GeV} < M_{h^0} < 350$ GeV
$\gamma\gamma \to H, A \to b\bar{b}$	$\mathcal{MSSM}$ heavy Higgs, for intermediate $\tan\beta$
$\gamma\gamma \to \tilde{f}\bar{\tilde{f}},\ \tilde{\chi}_i^+\tilde{\chi}_i^-,\ H^+H^-$	large cross sections, possible observations of FCNC
$\gamma\gamma \to S[\tilde{t}\bar{\tilde{t}}]$	$\tilde{t}\bar{\tilde{t}}$ stoponium
$\gamma e \to \tilde{e}^-\tilde{\chi}_1^0$	$M_{\tilde{e}^-} < 0.9 \times 2E_0 - M_{\tilde{\chi}_1^0}$
$\gamma\gamma \to W^+W^-$	anomalous W interactions, extra dimensions
$\gamma e^- \to W^-\nu_e$	anomalous W couplings
$\gamma\gamma \to WWWW$,$WWZZ$	strong WW scatt., quartic anomalous W, Z couplings
$\gamma\gamma \to t\bar{t}$	anomalous top quark interactions
$\gamma e^- \to \bar{t}b\nu_e$	anomalous Wtb coupling
$\gamma\gamma \to$ hadrons	total $\gamma\gamma$ cross section
$\gamma e^- \to e^-X$ and $\nu_e X$	$\mathcal{N}C$ and $\mathcal{C}C$ structure functions (polarized and unpolarized)
$\gamma g \to q\bar{q},\ c\bar{c}$	gluon distribution in the photon
$\gamma\gamma \to J/\psi\, J/\psi$	QCD Pomeron

new particles in supersymmetric and other extentions of the Standard Model. The accuracy of the precision measurements of anomalous W boson and top quark couplings will be improved significantly, complementing measurements at the e^+e^- mode of the linear collider.

Acknowledgements

We greatly acknowledge our colleagues for numerous and useful discussions on the various problems and topics. E.B. and I.G. thanks the Organizing Committee of the Workshop for kind hospitality and financial support. The work of E.B. was partly supported by the RFBR-DFG 99-02-04011, RFBR 00-01-00704, and CERN-INTAS 99-377 grants. I.G. is grateful to RFBR (grants 99-02-17211 and 00-15-96691) for support. I.W. is supported in part by the Grant-in-Aid for Scientific Research (No. 11640262) and the Grant-in-Aid for Scientific Research on Priority Areas (No. 11127205) from the Ministry of Education, Science and Culture, Japan. J.K. was partially supported by the EU Fourth Framework Programme 'Training and Mobility of Researchers', Network 'Quantum Chromodynamics and the Deep Structure of Elementary Particles', contract FMRX–CT98–0194.

References

[1] *Zeroth-Order Design Report for the Next Linear Collider* LBNL-PUB-5424, SLAC Report 474, May 1996.

[2] *Conceptual Design of a 500 GeV Electron Positron Linear Collider with Integrated X-Ray Laser Facility* DESY 97-048, ECFA-97-182.

[3] *JLC Design Study*, KEK-REP-97-1, April 1997.

[4] R.W. Assmann *et al.*, "*A 3-TeV e^+e^- linear collider based on CLIC technology,*" CERN-2000-008.

[5] I. Ginzburg, G. Kotkin, V. Serbo and V. Telnov, *Pizma ZhETF*, **34** (1981) 514; *JETP Lett.* **34** (1982) 491. Preprint INP 81-50, 1981, Novosibirsk.

[6] I. Ginzburg, G. Kotkin, V. Serbo and V. Telnov, *Nucl. Instr. & Meth.* **205** (1983) 47, Preprint INP 81-102, 1991, Novosibirsk.

[7] I. Ginzburg, G. Kotkin, S. Panfil, V. Serbo and V. Telnov, *Nucl. Instr.& Meth.* **219** (1984) 5.

[8] V. Telnov, *Nucl. Instr. & Meth.* **A294** (1990)72.

[9] V. Telnov, *Proc. of the Workshop on Physics and Experiments with Linear Colliders*, Saariselka, Finland, 1991, Ed. R.Orava et al., World Scientific, 1992.

[10] D. Borden, D. Bauer and D. Caldwell, *SLAC-PUB*-5715, *UCSD-HEP*-92-01.

[11] I.F. Ginzburg, *Proc. IX International Workshop on Photon – Photon Collisions*, San Diego, 1992, World Scientific.

[12] V. Telnov, *Proc. of IX International Workshop on Photon Photon Collisions*, San Diego, 1992, World Scientific.

[13] V. Telnov, *Nucl. Instr.& Meth.* **A355** (1995) 3.

[14] S. Brodsky and P. Zerwas, *Proc.of Workshop on Gamma-Gamma Colliders,* Berkeley CA, USA, 1994; *Nucl.Instr.&Meth.* **A355** (1995) 19.

[15] M. Baillargeon, G. Belanger and F. Boudjema, Proc. of the *"Two-Photon Physics from $DA\Phi NE$ to LEP200 and Beyond"*, Paris, 1994, ENSLAPP-A-473-94, hep-ph/9405359.

[16] D.Miller, *Proc. of Workshop on Phys. and Exper. with Linear Colliders,* 1995, Morioka-Appi, Japan.

[17] M. Baillargeon et al., *DESY 96–123D* (1996) 229.

[18] V. Telnov, *Int. J. Mod. Phys.* **A 13** (1998) 2399, hep-ex/9802003.

[19] V. Telnov, *Proc. of the International Conference on the Structure and Interactions of the Photon (Photon 99)*, Freiburg, Germany, 23-27 May 1999, Nucl. Phys. Proc. Suppl., **82** (2000) 359, hep-ex/9908005.

[20] I. Watanabe *et al.*, "$\gamma\gamma$ Collider as an Option of JLC", KEK Report 97-17, 1998.

[21] R. Brinkmann et al., *Nucl. Instr. &Meth.* **A406** (1998) 13.

[22] A. Sessler, Physics Today, **51** (1998) 48.

[23] V.I. Telnov, Photon colliders at TESLA, *Talk at Intern. Workshop on High Energy Photon Colliders*, Hamburg, 2000, to be published in *Nucl. Instr. Meth.* A, hep-ex/0010033.

[24] *Proc. of Workshop on $\gamma\gamma$ Colliders*, Berkeley CA, USA, 1994, *Nucl. Instr. &Meth.* **A355** (1995).

[25] *Intern. Workshop on High Energy Photon Colliders*, To be published in Nucl. Instrum. Meth. A, http://www.desy.de/~gg2000.

[26] R. Brinkmann, TESLA 99-15, *Proc. of 4th International Workshop on Physics and Experiments at Linear Colliders* (LCWS 99), Sitges, 1999.

[27] M.E. Peskin, SLAC-PUB-8288, 1999, *Proc. of 4th International Workshop on Physics and Experiments at Linear Colliders (LCWS 99), Sitges, 1999.* hep-ph/9910521; P.M. Zerwas, *Proc. of the 5th Intern. Workshop on Physics and Experiments at Linear Colliders (LCWS2000)*, FNAL, 2000.

[28] ECFA/DESY LC Physics Working Group: E. Accomando, *et al.*, *Phys. Rept.* **299** (1998).

[29] J. Bagger *et al.*, American Linear Collider Working Group, SLAC-PUB-8495, BNL-67545, FERMILAB-PUB-00-152, LBNL-46299, UCRL-ID-139524, LBL-46299, 2000, hep-ex/0007022.

[30] B. Pietrzyk, *The Global Fit to Electroweak Data*, *XXXth International Conference on High Energy Physics*, Osaka, 2000, http://www.ichep2000.rl.ac.uk/.

[31] I. Ginzburg and V. Serbo, *Proc. 23 Winter school of LINP*, v.2 (1988) 132.

[32] P. Igo-Kemenes, for the LEP Working Group on Higgs boson search, *Talk at the LEPC Open Session on Nov. 2000,* http://lephiggs.web.cern.ch/LEPHIGGS/talks/index.html

[33] ALEPH Collaboration (R. Barate et al.), CERN-EP-2000-138, Nov 2000, hep-ex/0011045; L3 Collaboration (M. Acciarri et al.), CERN-EP-2000-140, Nov 2000, to be published in *Phys. Lett.* **B**, hep-ex/0011043.

[34] S. Heinemeyer, W. Hollik and G. Weiglein, *Eur. Phys. J.* **C9** (1999) 343; H.E. Haber, *Proc. of 4th Int. Symposium on Radiative Corrections*, Barcelona, Spain, hep-ph/9901365.

[35] T. Barklow, *Proc. of the 1990 DPF Summer Study on High Energy Physics: "Research Directions for the Decade"*, Editor E. Berger, Snowmass, CO, 1990.

[36] J.F. Gunion and H.E. Haber, *Proceedings of the 1990 DPF Summer Study on High-Energy Physics: "Research Directions for the Decade"*, Editor E. Berger, Snowmass, CO, 1990; *Phys. Rev.* **D48** (1993) 5109.

[37] D.L. Borden, D.A. Bauer and D.O. Caldwell, *Phys. Rev.* **D48** (1993) 4018.

[38] T. Ohgaki *Int. J. Mod. Phys.* **A 15** (2000) 2587.

[39] V.Telnov, *Proc. of 17 th Intern. Conference on High Energy Accelerators (HEACC98)*, Dubna, Russia, 1998, KEK preprint 98-163, e-print: hep-ex/9810019.

[40] J.F. Gunion, L. Poggioli, R. Van Kooten, C. Kao and P. Rowson, *Proc. of the 1996 DPF/DPB Summer Study on "New Directions in High Energy Physics" (Snowmass96)*, 1996, Snowmass, Colorado, 1997, UCD-97-5, hep-ph/9703330.

[41] A. Djouadi, V. Driesen, W. Hollik and J.I. Illana, *Eur. Phys. J.* **C1** (1998) 149.

[42] B. Grzadkowski and J.F. Gunion, *Phys. Lett.* **B291**, 361 (1992).

[43] J.F. Gunion and J.G. Kelly, *Phys. Lett.* **B333**, 110 (1994).

[44] M. Krämer, J. Kühn, M.L. Stong and P.M. Zerwas, *Z. Phys.* **C64**, (1994) 21.

[45] S. Söldner-Rembold, J. Jikia, *Talk at Intern. Workshop on High Energy Photon Colliders*, Hamburg, 2000, to be published in *Nucl. Instr. Meth.* A, hep-ex/0101056; M. Melles, W.J. Stirling and V.A. Khoze, *Phys. Rev.* D61 (2000) 054015.

[46] T. Ohgaki, T. Takahashi and I. Watanabe, *Phys. Rev.* **D56** (1997) 1723.

[47] T. Ohgaki, T. Takahashi, I. Watanabe and T. Tauchi, *Int. J. Mod. Phys.* **A13** (1998) 2411.

[48] M. Melles, *Talk at Intern. Workshop on High Energy Photon Colliders*, Hamburg, 2000, to be published in *Nucl. Instr. Meth.* A, hep-ph/0008125; *Nucl. Phys. B (Proc. Suppl.)* **82** (2000) 379.

[49] K. Ispirian et al., *Yad. Fiz.* **11** (1970) 1278; *Sov. J. Nucl. Phys.* **11** (1970) 712.

[50] G. Jikia and A. Tkabladze, *Nucl. Instr. Meth.* **A355** (1995) 81; *Phys. Rev.* **D54** (1996) 2030.

[51] D.L. Borden, V.A. Khoze, W.J. Stirling and J. Ohnemus, *Phys. Rev.* **D50** (1994) 4499; V. Khoze, in *Proc. of Workshop "Photon'95",* Sheffield, UK, 1995.

[52] G. Jikia and S. Söldner-Rembold, *Nucl. Phys. B (Proc. Suppl.)* **82** (2000) 373.

[53] M. Melles and W.J. Stirling, *Phys. Rev.* **D59** (1999) 94009; *Eur. Phys. J.* **C9** (1999) 101; M. Melles, W.J. Stirling and V.A. Khoze, *Phys. Rev.* **D61** (2000) 54015.

[54] M. Melles and W.J. Stirling; *Nucl. Phys.* **B564** (2000) 325-342; *Eur. Phys.J.* **C9** (1999) 101, and *Phys. Rev.* **D59** (1999) 094009.

[55] M. Battaglia, *Proc.of 4th International Workshop on Physics and Experiments at Linear Colliders (LCWS 99)*, Sitges, 1999, hep-ph/9910271.

[56] I.F. Ginzburg and I.P. Ivanov, *Phys. Lett.* **B 408** (1997) 325; E. Boos, V. Ilyin, D. Kovalenko, T. Ohl, A. Pukhov, M. Sachwitz and H.J. Schreiber, *Phys. Lett.* **B427** (1998) 189; *Proc. of 4th Intern. Workshop on Physics and Experiments at Linear Colliders (LCWS 99)*, Sitges, 1999.

[57] G. Jikia, *Phys. Lett.* **B298** (1993) 224; *Nucl. Phys.* **B405** (1993) 24; M.S. Berger *Phys. Rev.* **D48** (1993) 5121; D.A. Dicus and C. Kao, *Phys. Rev.* **D49** (1994) 1265.

[58] E. Boos, J.C. Brient, D.W. Reid, H.J. Schreiber and R. Shanidze, DESY-00-162, 2000, hep-ph/0011366; D. Reid, *Proc. of 4th Intern. Workshop on Physics and Experiments at Linear Colliders (LCWS 99)*, Sitges, 1999.

[59] G. Borisov and F. Richard, *Proc. of 4th Intern. Workshop on Physics and Experiments at Linear Colliders (LCWS 99)*, Sitges, 1999, hep-ph/9905413.

[60] K. Desch and N. Meyer, ECFA-DESY LC-Workshop, Obernai, 16/10/99, http://ireswww.in2p3.fr/ires/ecfadesy/talks/desch/desch_fusion.ps.

[61] M. Mühlleitner, *Talk at Intern. Workshop on High Energy Photon Colliders*, Hamburg, 2000, to be published in *Nucl. Instr. Meth.* A.

[62] M.M. Mühlleitner, M. Krämer, M. Spira and P.M. Zerwas, DESY 00-198, hep-ph/0101083.

[63] ATLAS Coll., *Technical Design Report*, CERN–LHCC 99–14 (May 1999); CMS Coll., *Technical Proposal*, CERN–LHCC 94–38 (Dec. 1994).

[64] A. Djouadi et al., *Z. Phys.* **C74** (1997) 93; E. Accomando et al., *Phys. Rep.* **299** (1998) 1; P.M. Zerwas, *Proc., 1999 Cargèse Lectures,* hep-ph/0003221.

[65] M. Mühlleitner, PhD thesis, DESY-THESIS-2000-033, hep-ph/0008127.

[66] E. Asakawa, *Proc. of 4th Intern. Workshop on Physics and Experiments at Linear Colliders (LCWS99)*, Sitges, 1999. *Nucl. Instrum. Methods* **A**; E. Asakawa, J. Kamoshita, A. Sugamoto and I. Watanabe, *Eur. Phys. J.* **C14**, 335 (2000).

[67] C.N. Yang, *Phys. Rev.* **77**, 242 (1950).

[68] S.Y. Choi and K. Hagiwara, *Phys. Lett.* **B359**, 369 (1995).

[69] G. Jikia, *Talk at Intern. Workshop on High Energy Photon Colliders,* Hamburg, 2000, to be published in *Nucl. Instr. Meth.* A. G. Jikia and A. Tkabladze, hep-ph/0004068.

[70] A.T. Banin, I.F. Ginzburg and I.P. Ivanov, *Phys. Rev.* **D 59** (1999) 115001; I.F. Ginzburg and I.P. Ivanov, hep-ph/0004069.

[71] I.F. Ginzburg, M. Krawczyk and P. Olsand, *Talk at Intern. Workshop on High Energy Photon Colliders,* Hamburg, 2000, to be published in *Nucl. Instr. Meth.* A. G. Jikia and A. Tkabladze, hep-ph/0004068. and extended version in *Proc. LCWS2000*, FNAL, 2000.

[72] E. Asakawa, S.Y. Choi, K. Hagiwara and J.S. Lee, hep-ph/0005313.

[73] M. Klasen, *Talk at Intern. Workshop on High Energy Photon Colliders,* Hamburg, 2000, to be published in *Nucl. Instr. Meth.* A, hep-ph/0008082.

[74] T. Mayer, *Talk at Intern. Workshop on High Energy Photon Colliders,* Hamburg, 2000, to be published in *Nucl. Instr. Meth.* A, hep-ph/0009048.

[75] F. Cuypers, G.J.van Oldenborgh and R. Rückl, *Nucl. Phys.* **B383** (1992) 45; and **409** (1993) 128; F. Cuypers, *Phys. Rev.* **D49** (1994) 3075.

[76] A. Goto and T. Kon, *Europhys. Lett.* **19**, 575 (1992); T. Kon and A. Goto, *Phys. Lett.* **B295**, 324 (1995).

[77] C. Blöchinger, H. Fraas, LC-TH-2000-017. C. Blöchinger, F.Franke, H. Fraas, *Proc. Intern. Workshop on High-Energy Photon Colliders*, Hamburg, Germany, 14-17 Jun 2000. Submitted to Nucl. Instr. Meth. A, hep-ph/0008167.

[78] D.S. Gorbunov, V.A. Ilyin and V.I. Telnov, *Talk at Intern. Workshop on High Energy Photon Colliders*, Hamburg, 2000, to be published in *Nucl. Instr. Meth.* A, hep-ph/0012175.

[79] G. Bella *et al.,* (LEP TGC Working Group), LEPEWWG/TGC/2000-01, 2000; B. Abbott *et al.* (D0 Collaboration), *Phys. Rev.* **D60** (1999) 072002.

[80] For a review, see H. Aihara *et al.* in *Electroweak Symmetry Breaking and Beyond the Standard Model*, ed. T. Barklow et al., World Scientific, Singapore, 1995.

[81] For a few of the early references, see, for example E. Yehudai, *Phys. Rev.* **D41** (1990) 33 and *Phys. Rev.* **D44** (1991) 3434; S.Y. Choi and F. Schrempp, *Phys. Lett.* **B272** (1991) 149; S.J. Brodsky, T.G. Rizzo and I. Schmidt, *Phys. Rev.* **D52** (1995) 4929.

[82] M. Baillargeon, G. Belanger and F. Boudjema, *Nucl. Phys.* **B500** (1997) 224.

[83] T. Takahashi, *Proc. of Workshop on Physics and Experiments with Linear colliders*, Morioka-Appi, 1996, World Scientific.

[84] I.F. Ginzburg, *Proc. Workshop on Physics and Experiments with e^+e^- Linear Colliders*, Waikoloa, 1993.

[85] I.F. Ginzburg, V.A. Ilyin, A.E. Pukhov, V.G. Serbo and S.A. Shichanin, *Sov. Yad.Fiz.* **56** (1993) 57.

[86] I.F. Ginzburg, *Nucl. Instr. Meth.* **A 355** (1995) 63.

[87] I.F. Ginzburg, *Talk at Intern. Workshop on High Energy Photon Colliders,* Hamburg, 2000, to be published in *Nucl. Instr. Meth.* A.

[88] F. Boudjema, Convener's talk (W Working group), *1st Meeting of the Workshop on e^+e^- Collisions at 500 GeV: The Physics Potential*, Munich-Annecy-Hamburg, Munich, 1992; M. Baillargeon, G. Belanger, and F. Boudjema, ENSLAPP-A-473-94, 1994.

[89] S.J. Brodsky, in Physics and Experiments with Linear e^+e^- Colliders, Waikoloa, 1993, ed. F.A. Harris *et al.*, World Scientific.

[90] G. Jikia, *Nucl. Instr. & Meth.* **A355** (1995) 84; *Nucl. Phys.* **B437** (1995) 520.

[91] K. Cheung, *Phys. Lett.* **B323** (1994) 85; *Phys. Rev.* **D50** (1994) 4290.

[92] K. Hagiwara, I. Watanabe and P.M. Zerwas, *Phys. Lett.* **B278** (1992) 187.

[93] N. Arkani-Hamed, S. Dimopoulos and G. Dvali, *Phys. Lett.* **B429** (1998) 263 and *Phys. Rev.* **D59** (1999) 086004; I. Antoniadis, N. Arkani-Hamed, S. Dimopoulos and G. Dvali, *Phys. Lett.* **B436** (1998) 257.

[94] G.F. Giudice, R. Rattazzi and J.D. Wells, *Nucl. Phys.* **B544** (1999) 3; T. Han, J.D. Lykken and R. Zhang, *Phys. Rev.* **D59**, (1999) 105006, E.A. Mirabelli, M. Perelstein and M.E. Peskin, *Phys. Rev. Lett.* **82** (1999) 2236; J.L. Hewett, *Phys. Rev. Lett.* **82**, (1999) 4765; for a review see T.G. Rizzo, hep-ph/9910255.

[95] T.G. Rizzo, *Talk at Intern. Workshop on High Energy Photon Colliders, Hamburg*, 2000, to be published in *Nucl. Instr. Meth.* A, hep-ph/0008037.

[96] T. Rizzo, *Phys. Rev.* **D60** (1999) 115010, hep-ph/9904380.

[97] K.Cheung, *Phys. Rev*, **D61** (2000) 015005.

[98] H.Davoudiasl, *J. Mod. Physics* **A15** (2000) 2613.

[99] R.D. Peccei and X. Zhang, *Nucl. Phys.* **B337** (1990) 269; R.D. Peccei, S. Peris and X. Zhang, *Nucl. Phys.* **B349** (1991) 305.

[100] J.L. Hewett, *Int.J.Mod.Phys.* **A13** (1998) 2389.

[101] J.H. Kühn, *Act.Phys.Pol.* **B12** (1981) 347; I.Bigi, Y. Dokshitzer, V. Khoze, J. Kühn, P. Zerwas, *Phys. Lett.* **B181** (1986) 157; V. Fadin and V. Khoze, *JETP Lett.* **46** (1987) 525; J. Strassler and M.Peskin, *Phys. Rev.* **D34** (1991) 1500; see the last review on the subject and references therein, A.H. Hoang et al., *Eur.Phys.J.* **C3** (2000) 1.

[102] A.A. Penin and A.A. Pivovarov, *Nucl.Phys.* **B550** (1999) 375.

[103] E. Boos, *Talk at Intern. Workshop on High Energy Photon Colliders, Hamburg,* 2000, to be published in *Nucl. Instr. Meth.* A.

[104] A. Djouadi, J. Ng, T.G. Rizzo et al. hep-ph/9504210, Report-no: SLAC-PUB-95-6772, GPP-UdeM-TH-95-17, TRI-PP-95-05.

[105] P. Poulose and S.D. Rindani, *Phys. Lett.* **B452** (1999) 347.

[106] S.Y. Choi and K. Hagiwara, *Phys. Lett.* **B359** (1995) 369; M.S. Baek, S.Y. Choi and C.S. Kim, *Phys. Rev.* **D56** (1997) 6835.

[107] E. Boos, M. Dubinin, A. Pukhov, M. Sachwitz and H.J. Schreiber, in preparation.

[108] G.V. Jikia, *Nucl. Phys.* **B374** (1992) 83; E.Yehudai, *Proc. of 2nd International Workshop on Physics and Experiments with Linear e^+e^- Colliders, Waikoloa* 1993, hep-ph/9308281; E. Boos, A. Pukhov, M. Sachwitz, H.J. Schreiber, *Talk at Joint ECFA / DESY Study: Physics and Detectors for a Linear Collider, Hamburg, 1996*, hep-ph/9711253; E.Boos, A. Pukhov, M. Sachwitz, H.J. Schreiber, *Phys. Lett.* **B404** (1997) 119; J.-J. Cao, J.-X. Wang, J. Yang, B.L. Young and X.Zhang, *Phys. Rev.* **D58** (1998) 094004.

[109] E. Boos, L. Duduko and T. Ohl, *Eur. Phys. J.* **C11** (1999) 473.

[110] E. Boos, M. Dubinin, M. Sachwitz and H. J. Schreiber *Eur. Phys.J.* **C16** (2000) 269.

[111] R. Godbole and G. Pancheri, *Talk at Intern. Workshop on High Energy Photon Colliders,* Hamburg, 2000, to be published in *Nucl. Instr. Meth.* A, hep-ph/0101320.

[112] I.F. Ginzburg, S.L. Panfil and V.G. Serbo, Nucl.Phys. **B284** (1987) 685; **B296** (1988) 569; G.D. Ivanov, V. and Serbo, *Phys. At. Nucl.* **56** (1993) 45.

[113] A. Vogt, *Nucl. Phys. B Proc. Suppl.* **82** (2000) 394.

[114] A. Gehrmann-De Ridder, H. Spiesberger and P.M. Zerwas, *Phys. Lett.* **B469** (1999) 259.

[115] P. Aurenche et al., *Prog. Theor. Phys.*, **92** (1994) 175, hep-ph/9401269.

[116] M. Klasen, T. Kleinwort, and G. Kramer, *Eur. Phys. J. Direct*, **C1** (1998) 1, hep-ph/9712256.

[117] M. Drees, M. Krämer, J. Zunft, and P. Zerwas. *Phys. Lett.*, **B306** (1993) 371.

[118] T. Wengler and A. De Roeck, hep-ph/0010293. *Talk at Intern. Workshop on High Energy Photon Colliders*, Hamburg, 2000, to be published in *Nucl. Instr. Meth.* A.

[119] P. Jankowski, M. Krawczyk and A. De Roeck, *Talk at Intern. Workshop on High Energy Photon Colliders*, Hamburg, 2000, to be published in *Nucl. Instr. Meth. A*.

[120] M. Stratmann and W. Vogelsang, *Phys. Lett.* **B386** (1996) 370; M. Stratmann, *Nucl. Phys. Proc. Suppl.* **82** (2000) 400.

[121] J. Kwiecinski and B. Ziaja, *Talk at Intern. Workshop on High Energy Photon Colliders,* Hamburg, 2000, to be published in *Nucl. Instr. Meth.* A, hep-ph/0006292.

[122] J. Kwieciński and L. Motyka, *Phys. Lett.* **B438** (1998) 203; J. Kwieciński, L. Motyka and A. De Roeck, hep-ph/0001180.

[123] I.F. Ginzburg and D.Yu. Ivanov, *Phys. Lett.* **B276** (1992) 214.

[124] J. Blümlein and A. Kryukov, DESY-99-072, *Talk at Intern. Workshop on High Energy Photon Colliders*, Hamburg, 2000, to be published in *Nucl. Instr. Meth.* A; hep-ph/0008097; A. Zarnecki, ibid, hep-ph/0006335.

[125] I.F. Ginzburg and S.L. Panfil, *Sov. J. Nucl. Phys.* **36** (1982) 850; I.F. Ginzburg and A. Schiller, *Phys. Rev.* **D60** (1999) 075016.